



ELSEVIER

Nuclear Physics A 636 (1998) 427–451

NUCLEAR
PHYSICS A

Temperature dependence of quantal and thermal dampings of the hot giant dipole resonance

Nguyen Dinh Dang¹, Akito Arima

Cyclotron Laboratory, RIKEN, Wako, Saitama 351-01, Japan

Received 10 October 1997; revised 30 March 1998; accepted 14 April 1998

Abstract

A systematic study of the damping of the giant dipole resonance (GDR) in ^{90}Zr , ^{120}Sn and ^{208}Pb as a function of temperature T is performed. The double-time Green function technique is employed to determine the single-particle and GDR dampings. The single-particle energies, obtained in the Woods–Saxon potential for these nuclei, are used in the calculations. The results show that the coupling of collective vibration to the pp and hh excitations, which causes the thermal damping width, is responsible for the enlargement of the total width with increasing temperature up to $T \approx 3$ MeV and its saturation at higher temperatures. The quantal width, which arises from the coupling of the collective mode to the ph excitations decreases slowly with increasing temperature. The effect of single-particle damping on the GDR width is small. The results are found in an overall agreement with the experimental data for the GDR width, obtained in the inelastic α scattering and heavy-ion fusion reactions at excitation energies $E^* \leq 450$ MeV. At high excitation energies ($E^* > 400$ MeV) a behavior similar to the transition from zero to ordinary sounds is observed. © 1998 Elsevier Science B.V.

PACS: 21.10.Pc; 24.10.Pa; 24.30.Cz

Keywords: Single-particle levels and strength functions; Thermal and statistical models; Giant resonances

1. Introduction

The study of the giant dipole resonance (GDR), built on compound nuclear states (hot GDR), has been the subject of a considerable number of experimental and theoretical

¹ Present address: Department of Physics (Research Building, 2F), Faculty of Science, Saitama university, 255 Shimo-Okubo, 388-8570 Saitama, Japan. E-mail: dang@rikexp.riken.go.jp. On leave of absence from the Institute of Nuclear Science and Technique, VAEC, Hanoi, Vietnam.

efforts during the last fifteen years (See Refs. [1,2] for the reviews). The main issue of many debates on the hot GDR phenomenon can be summarized as follows. The energy of the hot GDR is about the same as of the one built on the ground state (the g.s. GDR) and can be well described within the framework of existing theories. However, its width increases rapidly with increasing the excitation energy E^* (or temperature T) up to around 130 MeV in Sn isotopes. At higher excitation energies the width increases slowly and even saturates.

Most important information about the behavior of the hot GDR has been extracted so far from the compound-nuclear reactions induced in heavy-ion collisions [3–9]. In these experiments the hot compound nucleus was usually formed at high angular momentum. The dependence of the width of the hot GDR as a function of the excitation energy E^* contains then both effects of the angular momentum and the temperature. Recently two new experimental methods, involving compound nuclear reactions [10] and inelastic α scattering [11], have been undertaken. In Ref. [10] large arrays of γ detectors have been set up to measure the GDR of a hot system at a definite angular momentum. Ref. [11] introduced a new technique using α particles to excite the target nucleus via inelastic scattering at a small angular momentum. These methods have opened a possibility to study individually the effects due to thermal fluctuations and due to angular momentum on the damping of the hot GDR in a direct comparison with theoretical predictions.

From the microscopic point of view the g.s. GDR ($T = 0$) can be represented within the random phase approximation (RPA) as one or a group of several collective phonons, each of which is a coherent superposition of ph excitations. Once this picture is established, the phonons can be considered as undamped harmonic oscillators. An accurate description of the energy and sum rule of the g.s. GDR has been achieved within the RPA. The RPA cannot account for the width of the GDR except for some Landau splitting [12–15], which turns out to be rather stable against temperature [12,14,15]. The g.s. GDR acquires an escape width Γ^\uparrow via a direct γ or particle emission and a spreading width Γ^\downarrow by coupling to more complicated configurations beyond the RPA. The latter can be described via the coupling of one-phonon to two-phonon states as in the quasiparticle-phonon model (QPM) [16], to “ $1p1h \otimes$ phonon”-configurations as in the nuclear-field theory (NFT) [17] or directly to $2p2h$ -configuration mixing as in the second RPA (SRPA) [18] and extended SRPA [19]. Since such kind of coupling is purely a quantal effect, the spreading width Γ^\downarrow is also called the quantal width Γ_Q . The extension of such a description to $T \neq 0$ has shown a little change of Γ^\downarrow [20,21]. As concerned the escape width, its value is relatively small (within hundreds keV) for the g.s. GDR. The stability of the dipole response function against varying the temperature in the self-consistent RPA calculations by Sagawa and Bertsch [14], including the unbound continuum in the space for the particle states, is a clear demonstration that the escape width of the GDR is mostly independent of temperature. Hence the source of the increase of the hot GDR’s width in the temperature interval $0 \leq T \leq 5-6$ MeV must come mainly from the thermal effects. In finite systems such as nuclei thermal effects increase, while quantal effects are expected to decrease with increasing temperature. So far most thermal effects have been included via the thermal fluctuations of nuclear

shapes [22,23]. They have also been taken into account in the recent theory on the hot GDR's width [24]. The authors of Ref. [9] have pointed out, however, that the increase of the width, offered by the theory in Ref. [24], is still quite slow in order to account for the experimental systematics. Ref. [9], therefore, has called for a search of a missing effect, emphasizing the role played by thermal and angular momentum effects in the low excitation energy region ($E^* \leq 200$ MeV). The most recent theoretical evaluations in Ref. [25], which include the thermal shape fluctuations within an adiabatic model, agree nicely with the α -scattering data in Ref. [11] for the GDR width in ^{120}Sn and ^{208}Pb at temperatures $1 \text{ MeV} < T \leq 3 \text{ MeV}$ ($30 \text{ MeV} \leq E^* \leq 130 \text{ MeV}$). The increase of the evaporation width Γ_{ev} due to a finite life-time of the compound nuclear states [26], has been also included to improve the results at $T \sim 3 \text{ MeV}$. The theoretical predictions of Ref. [25] are given for $T \leq 3.4 \text{ MeV}$, so the region of the width saturation ($E^* > 130 \text{ MeV}$), where a considerable number of heavy-ion fusion data has been accumulated up to $E^* \sim 450 \text{ MeV}$, is left out in this description. These achievements have also shown that the effects due to angular momentum on the data set of interest are negligible. The width of the GDR has been shown to depend noticeably on the angular momentum J only above a rather high value of $J \geq 35\hbar$ at $T \simeq 1.5\text{--}1.8 \text{ MeV}$ and only in a lighter nucleus ^{106}Sn [27]. The angular momentum effects are unimportant for $A \geq 120$.

From the macroscopic point of view, the g.s. GDR is an analogue of the Landau zero sound [28]. The damping of the hot GDR has been studied intensively within the framework of the Landau-Vlasov theory using the Landau integral including the collision term (See Refs. [29,30] and references therein). This approach and its further modification have shown a continuously increasing width of the GDR as increasing the temperature. The width saturation at $T \geq 3 \text{ MeV}$ and the "disappearance" of the GDR at high temperature ($T > 4.5\text{--}5 \text{ MeV}$), observed in the heavy-ion fusion experiments, is interpreted within this approach mainly as a result of an exceedingly large width. In the recent Ref. [31], it has been shown, however, that at $T \geq 2 \text{ MeV}$ the regime of rare collisions, where the RPA method can be applied in the theory of Fermi liquid, must be replaced with the regime of frequent collisions. Including the memory effects in the collisional integral and the quadrupole distortion of the Fermi surface, the collisional width of the GDR, obtained in Ref. [31], turns out to be rather independent of temperature in an agreement with the predictions of microscopic theories [20,21]. Thermal shape fluctuations have been also taken into account based on the Landau theory of nuclear shape transitions in Ref. [32]. The latter provides a nice macroscopic description of thermal fluctuations in all quadrupole shape degrees of freedom. With all parameters fixed at zero temperature this theory shows a good agreement with the data for hot GDR up to $T = 2\text{--}3 \text{ MeV}$.

In the present situation, of particular importance in the theories of the hot GDR is the understanding in a consistent and microscopic way the behavior of the the hot GDR as a function of temperature in a large interval. Such a theory must cover the region of the width's increase at low temperatures ($0 \leq T \leq 3 \text{ MeV}$) as well as the region of the width's saturation ($T \geq 3 \text{ MeV}$) up to the region where the GDR is thought to disappear ($T > 4.5\text{--}5 \text{ MeV}$). There are a number of questions to be answered, such as

the role of motional narrowing [33] in the saturation of the GDR at high temperature. The question of a phase transition, which seems to take place at around $E^* = 100$ MeV in tin isotopes in the recent theory in Ref. [24] due to the limitation of the maximal angular momentum, has also opened room for debates. A similar question arises in the semiclassical approaches on whether the saturation of the GDR width is a signature of the phase transition from zero to ordinary sounds in hot nuclei [30]. While there is no doubt that these issues cannot be answered in one work, they certainly have created a good motivation for our present study.

In the recent works [34,35] we have shown that the coupling of the RPA phonon to the pp and hh configurations, which appear at non-zero temperature, leads to the thermal damping of the phonon excitation. The contribution of the additional configurations at $T \neq 0$ in the increase of the Landau damping has also been studied in Ref. [36]. In the present paper we will elaborate further this concept, and perform a systematic study of the GDR width in ^{90}Zr , ^{120}Sn and ^{208}Pb as a function of temperature in comparison with recent experimental data from inelastic α scattering [11] as well as from heavy-ion fusion reactions [3–9]. This study over a wide range of temperatures, which includes both the region of the width's increase and width's saturation, allows us to draw conclusions on the role of the coupling to pp and hh in an accurate description of the GDR width in realistic hot nuclei. The formalism of the approach is presented in Section 2. Section 3 is devoted to the analysis and discussion of numerical results. The comparison with the experimental data as well as with other theoretical descriptions is discussed. A possible relation between the behavior of the GDR width in finite nuclei and the transition from zero to ordinary sounds in a Fermi liquid is also studied. The paper is summarized in the last section, where conclusions are provided.

2. Formalism

We consider a model Hamiltonian for the description of the coupling of collective oscillations (phonons) to the field of ph , pp and hh pairs in a form of a sum of three terms:

$$H = H_a + H_b + H_c. \quad (2.1)$$

The first term H_a is the field of independent single particles:

$$H_a = \sum_s E_s a_s^\dagger a_s, \quad (2.2)$$

where a_s^\dagger and a_s are creation and destruction operators of a particle or hole state with energy $E_s = \epsilon_s - \epsilon_F$ with ϵ_s being the single-particle energy and ϵ_F the Fermi surface's energy. Hereafter the energy E_s is also called the single-particle energy whenever there is no confusion with ϵ_s .

The second term H_b in Eq. (2.1) stands for the phonon field as the field of harmonic oscillators:

$$H_b = \sum_q \omega_q Q_q^\dagger Q_q, \quad (2.3)$$

where Q_q^\dagger and Q_q are the creation and destruction operators of a phonon with energy ω_q .

The last term H_c in Eq. (2.1) describes the coupling between the first two:

$$H_c = \sum_{ss'q} F_{ss'}^{(q)} a_s^\dagger a_{s'} (Q_q^\dagger + Q_q). \quad (2.4)$$

From now on the indices s and s' denote particle ($p, E_p > 0$) or hole ($h, E_h < 0$), while the index q is reserved for the phonon state $q = \{\lambda, i\}$ with multipolarity λ (the projection μ of λ in the phonon index is omitted in the writing for simplicity). The sum in Eq. (2.4) is carried over $\lambda \geq 1$. This form of the model Hamiltonian in Eqs. (2.1)–(2.4) is quite general and common in many microscopic approaches to nuclear collective excitations. The difference is in the way of defining the single-particle energy E_s , phonon energy ω_q and phonon structure under a specific effective coupling $F_{ss'}^{(q)}$. In the QPM [16] or NFT [17], e.g., the coupling vertex $F_{ss'}^{(q)}$ is a sum of products of the coupling strength and the coupling-matrix elements. The coupling strength contains the RPA amplitudes of ph configurations in the collective oscillation. The coupling matrix elements can be obtained through the derivative of the central potential. In the QPM, e.g., phonon operators Q_q^\dagger and Q_q have the fermion structure, being built from the coherent ph or quasiparticle pairs. The form in Eqs. (2.1)–(2.4) has been derived rigorously from the QPM Hamiltonian in Ref. [35]. In the simplest case when the two-body term consist of only a separable isovector dipole–dipole interaction, one recovers from Eqs. (2.1)–(2.4) the Hamiltonian, widely used in the literature to describe the g.s. GDR [37]. There is only one term, which is omitted in Eq. (2.1). This term is a sum of products of two pp (hh) pairs. In the literature this term is also called the scattering term. It represents the interparticle interactions, which are not included in the particle–phonon couplings H_c in Eq. (2.4). As it contains no coupling to one-phonon terms, it has a little influence on the damping of phonon excitations built at $T = 0$. Indeed, the estimation in Ref. [38] has shown that the effect caused by this term to the phonon energies is negligible within the RPA except for very low-lying states in transitional nuclei. This is the reason why in the description of the multipole g.s. giant resonances in the QPM [16], this term was always neglected (See, e.g., Ref. [39]). Our interest in the present paper is to study the damping of the collective mode, generated by phonon operators via its coupling to the single-particle field at non-zero temperature. Therefore, we also neglect this scattering term at $T \neq 0$. Meanwhile, it should be noticed that as the excitation energy and level density increase, the residual interaction becomes more and more important. Incoherent collision-like processes and anharmonicity of collective modes lead to the stochastization of actual stationary states, which also contributes in the saturation of the width of the GDR at high temperatures. This question has been studied in detail by Zelevinsky et al. in Ref. [40], where the damping of GDR in highly excited nuclei was considered within the chaotic dynamics.

We derive the main equations of the formalism, making use of the temperature-dependent double-time Green functions [41–43]. This method has been proved to be very convenient for application in statistical systems as the advanced and retarded double-time Green functions can be analytically continued in the complex-energy plane, which facilitate the explicit derivation of the single-particle and phonon dampings.

Let us introduce the following double-time Green functions, which describe:

(i) *The propagation of a free particle (or hole):*

$$G_{s';s}(t-t') = \langle\langle a_{s'}(t); a_s^\dagger(t') \rangle\rangle, \quad (2.5)$$

(ii) *The propagation of a free phonon:*

$$G_{q';q}(t-t') = \langle\langle Q_{q'}(t); Q_q^\dagger(t') \rangle\rangle, \quad (2.6)$$

(iii) *The particle–phonon coupling in the single-particle field:*

$$\Gamma_{s'q;s}^-(t-t') = \langle\langle a_{s'}(t) Q_q(t); a_s^\dagger(t') \rangle\rangle, \quad (2.7)$$

$$\Gamma_{s'q;s}^+(t-t') = \langle\langle a_{s'}(t) Q_q^\dagger(t); a_s^\dagger(t') \rangle\rangle, \quad (2.8)$$

(iv) *The transition between a nucleon pair and a phonon:*

$$\mathcal{G}_{ss';q}^-(t-t') = \langle\langle a_s^\dagger(t) a_{s'}(t); Q_q^\dagger(t') \rangle\rangle, \quad (2.9)$$

In Eqs. (2.5)–(2.9) the standard notation for the double-time retarded Green function is used:

$$G(t-t') = \langle\langle A(t); B(t') \rangle\rangle \equiv -i\theta(t-t') \langle[A(t), B(t')]_{\pm}\rangle, \quad (2.10)$$

where $[A(t), B(t')]_{\pm} = (A(t)B(t') - \eta B(t')A(t))$ with $\eta = 1$ if A and B are boson and -1 if A and B are fermion operators; $\langle \dots \rangle$ denotes the average over the the grand canonical ensemble:

$$\langle \dots \rangle = \frac{\text{Tr}(\dots \exp(-\beta H))}{\text{Tr}(\exp(-\beta H))}, \quad \beta = T^{-1}, \quad (2.11)$$

Applying now the standard method of the equation of motion for the double-time Green function [42,43], we obtain a set of coupled equations for an hierarchy of double-time Green functions. Apart from the functions in Eqs. (2.5)–(2.9), this hierarchy contains also higher-order ones. In order to close the set to the functions in Eqs. (2.5)–(2.9), we employ the following decoupling approximation, which is originated from the approximate second quantization [41] and improved thermodynamically for the non-zero temperature case:

$$\langle\langle \underbrace{a_{s_1} Q_q^\dagger Q_{q'}}_{\text{decoupled}}; a_s^\dagger \rangle\rangle = \delta_{qq'} \nu_q G_{s_1;s}, \quad \langle\langle \underbrace{a_{s_1} Q_{q'} Q_q^\dagger}_{\text{decoupled}}; a_s^\dagger \rangle\rangle = \delta_{qq'} (1 + \nu_q) G_{s_1;s}, \quad (2.12)$$

$$\langle\langle \underbrace{a_s^\dagger a_{s_1}}_{\text{decoupled}} (Q_{q'}^\dagger + Q_{q'}); Q_q^\dagger \rangle\rangle = \delta_{ss_1} n_s G_{q';q}, \quad \langle\langle \underbrace{a_{s'} a_{s_1}^\dagger}_{\text{decoupled}} a_{s_1}; a_s^\dagger \rangle\rangle = \delta_{s's_1} (1 - n_{s'}) G_{s';s}. \quad (2.13)$$

In Eqs. (2.12) and (2.13) $n_s = \langle a_s^\dagger a_s \rangle$ and $\nu_q = \langle Q_q^\dagger Q_q \rangle$ are the single-particle and phonon occupation numbers, respectively. The time variable is omitted for simplicity.

Making then the Fourier transformation to the energy plane E , we come to the following set of five equations for the Fourier transforms of the Green functions in Eqs. (2.5)–(2.9):

$$(E - E_s)G_s(E) - \sum_{q's'_1} F_{ss'_1}^{(q')} (\Gamma_{s'_1q';s}^-(E) + \Gamma_{s'_1q';s}^+(E)) = \frac{1}{2\pi}, \tag{2.14}$$

$$(E - \omega_q)G_q(E) - \sum_{s_1s'_1} F_{s_1s'_1}^{(q)} \mathcal{G}_{s_1s'_1;q}(E) = \frac{1}{2\pi}, \tag{2.15}$$

$$(E - E_{s'} - \omega_q)\Gamma_{s'q;s}^-(E) - (1 - n_{s'} + \nu_q) \sum_{s_1} F_{s'_1s_1}^{(q)} G_{s_1;s}(E) = 0, \tag{2.16}$$

$$(E - E_{s'} + \omega_q)\Gamma_{s'q;s}^+(E) - (n_{s'} + \nu_q) \sum_{s_1} F_{s'_1s_1}^{(q)} G_{s_1;s}(E) = 0, \tag{2.17}$$

$$(E - E_{s'} + E_s)\mathcal{G}_{ss';q}(E) - (n_s - n_{s'}) \sum_{q'} F_{s's'}^{(q')} G_{q';q}(E) = 0. \tag{2.18}$$

We notice that Eqs. (2.14) and (2.15) in this set are still exact. The last three equations are obtained within the decoupling scheme in Eqs. (2.12) and (2.13). This decoupling approximation is fairly coarse. For instance, it is insufficient to incorporate the higher-order incoherent correlations and anharmonicity, which may become significant at high excitation energies and level densities [40]. On the other hand it allows to reveal here the effect of thermal damping on the width of the GDR in a simple and transparent way. A part of these higher-order effects can be included if one takes higher-order Green functions in the hierarchy into account and then applies this decoupling scheme at the corresponding higher level. While it is obviously impossible to take into account the complete infinite hierarchy, the inclusion of many higher-order Green functions is already a formidable task for further studies. Functions $\Gamma^-(E)$, $\Gamma^+(E)$ and $\mathcal{G}(E)$ in the last three equations can be eliminated, being expressed in terms of $G_{s';s}(E)$ and $G_{q';q}(E)$. Inserting the results in the first two equations, we end up with a set of two equations for $G_{s';s}(E)$ and $G_{q';q}(E)$, which describe the particle (hole) and phonon propagations, respectively. The propagation of a single particle (or hole) state and the one of a single phonon state can be easily studied, limiting the consideration to the case with $G_{s;s}(E) \equiv G_s(E)$ ($s = s'$) and $G_{q;q}(E) \equiv G_q$ ($q = q'$). The equations in this case have a simple form:

$$G_s(E) = \frac{1}{2\pi} \frac{1}{E - E_s - M_s(E)}, \tag{2.19}$$

$$G_q(E) = \frac{1}{2\pi} \frac{1}{E - \omega_q - P_q(E)}. \tag{2.20}$$

The functions $M_s(E)$ and $P_q(E)$ are the mass and polarization operators by analogy with the quantum field theory:

$$M_s(E) = \sum_{q_1s_1} F_{ss_1}^{(q_1)} F_{s_1s}^{(q_1)} \left(\frac{\nu_{q_1} + 1 - n_{s_1}}{E - E_{s_1} - \omega_{q_1}} + \frac{n_{s_1} + \nu_{q_1}}{E - E_{s_1} + \omega_{q_1}} \right), \tag{2.21}$$

$$P_q(E) = \sum_{s_1 s'_1} F_{s_1 s'_1}^{(q)} F_{s'_1 s_1}^{(q)} \frac{n_{s_1} - n_{s'_1}}{E - E_{s'_1} + E_{s_1}}. \quad (2.22)$$

The mass and polarization operators $M_s(E)$ and $P_q(E)$ can be continued analytically in the complex-energy plane:

$$M_s(\omega \pm i\varepsilon) = M_s(\omega) \mp i\gamma_s(\omega), \quad (2.23)$$

$$P_q(\omega \pm i\varepsilon) = P_q(\omega) \mp i\gamma_q(\omega). \quad (2.24)$$

In Eqs. (2.23) and (2.24) $M_s(\omega)$ and $P_s(\omega)$ (ω is real) are real functions, which correspond to the real parts of $M_s(\omega \pm i\varepsilon)$ and $P_q(\omega \pm i\varepsilon)$, respectively

$$M_s(\omega) = \mathcal{P} \sum_{q_1 s_1} F_{s s_1}^{(q_1)} F_{s_1 s}^{(q_1)} \left(\frac{\nu_{q_1} + 1 - n_{s_1}}{\omega - E_{s_1} - \omega_{q_1}} + \frac{n_{s_1} + \nu_{q_1}}{\omega - E_{s_1} + \omega_{q_1}} \right), \quad (2.25)$$

$$P_q(\omega) = \mathcal{P} \sum_{s_1 s'_1} F_{s_1 s'_1}^{(q)} F_{s'_1 s_1}^{(q)} \frac{n_{s_1} - n_{s'_1}}{\omega - E_{s'_1} + E_{s_1}}. \quad (2.26)$$

The symbol \mathcal{P} indicates the principal value of the corresponding integral. As has been mentioned previously, closing the hierarchy to the functions in Eqs. (2.5)–(2.9) restricts the couplings in Eqs. (2.25) and (2.26) to at most $2p1h$ configurations if the one-phonon operator generates the collective ph excitation. On the other hand the g.s. GDR acquires the spreading width Γ^\dagger mostly via coupling to $2p2h$ configurations. The latter can be included by extending the hierarchy to higher-order Green functions of “ $1p1h \oplus$ phonon” type $\langle\langle a_h^\dagger(t) a_p(t) Q_q(t); Q_{q'}^\dagger(t') \rangle\rangle$ as in Ref. [20] or two-phonon type $\langle\langle Q_{q_1}(t) Q_{q_2}(t); Q_{q'}^\dagger(t') \rangle\rangle$, etc. as in Ref. [21]. The result would then include the graphs in Figs. 3 and 4 of Ref. [20] or in Fig. 1 of Ref. [21] for the phonon polarization operator $P_q(E)$. The numerical calculations in Refs. [20,21,44] have shown, however, that the effects of these graphs on the spreading width of the GDR are almost independent of the temperature. Therefore, in order to maintain the simplicity, we will include in the next section the spreading due to these effects in the parameters of the model defined at $T = 0$.

The imaginary parts $\gamma_s(\omega)$ and $\gamma_q(\omega)$ in Eqs. (2.23) and (2.24) play the role of the damping of particle (hole) and phonon states, respectively:

$$\gamma_s(\omega) = \pi \sum_{q_1 s_1} F_{s s_1}^{(q_1)} F_{s_1 s}^{(q_1)} \left[(\nu_{q_1} + 1 - n_{s_1}) \delta(\omega - E_{s_1} - \omega_{q_1}) + (n_{s_1} + \nu_{q_1}) \delta(\omega - E_{s_1} + \omega_{q_1}) \right], \quad (2.27)$$

$$\gamma_q(\omega) = \pi \sum_{s_1 s'_1} F_{s_1 s'_1}^{(q)} F_{s'_1 s_1}^{(q)} (n_{s_1} - n_{s'_1}) \delta(\omega - E_{s'_1} + E_{s_1}). \quad (2.28)$$

In Ref. [35] it has been proved in an example of a damped harmonic oscillator that the function $\gamma_q(\omega)$ in Eq. (2.28) is indeed the damping of the phonon state, while $P_q(\omega)$ gives its energy shift. A similar proof can be extended to the single-particle damping $\gamma_s(\omega)$ in Eq. (2.27).

Using the analytical continuations of the single-particle and phonon Green functions G_s and G_q , one can also derive the corresponding spectral intensities J_s and J_q from the relations [41]

$$G_s(\omega + i\varepsilon) - G_s(\omega - i\varepsilon) = -iJ_s(\omega)(\exp(\beta\omega) + 1), \tag{2.29}$$

$$G_q(\omega + i\varepsilon) - G_q(\omega - i\varepsilon) = -iJ_q(\omega)(\exp(\beta\omega) - 1). \tag{2.30}$$

The general form of the spectral intensities is proportional to the Lorentzian single-particle and phonon strength functions $S_s(\omega)$ and $S_q(\omega)$, respectively

$$J_s(\omega) = S_s(\omega)(\exp(\beta\omega) + 1)^{-1}, \quad S_s = \frac{1}{\pi} \frac{\gamma_s(\omega)}{(\omega - E_s - M_s(\omega))^2 + \gamma_s^2(\omega)}, \tag{2.31}$$

$$J_q(\omega) = S_q(\omega)(\exp(\beta\omega) - 1)^{-1}, \quad S_q = \frac{1}{\pi} \frac{\gamma_q(\omega)}{(\omega - \omega_q - P_q(\omega))^2 + \gamma_q^2(\omega)}. \tag{2.32}$$

The single-particle and phonon occupation numbers n_s and ν_q in Eqs. (2.16)–(2.18) are now defined as the Fermi–Dirac and Bose–Einstein distributions, which are smeared out with the half-widths γ_s and γ_q , respectively:

$$n_s = \frac{1}{\pi} \int_{-\infty}^{\infty} \frac{\gamma_s(\omega)(\exp(\beta\omega) + 1)^{-1}}{(\omega - E_s - M_s(\omega))^2 + \gamma_s^2(\omega)} d\omega, \tag{2.33}$$

$$\nu_q = \frac{1}{\pi} \int_{-\infty}^{\infty} \frac{\gamma_q(\omega)(\exp(\beta\omega) - 1)^{-1}}{(\omega - \omega_q - P_q(\omega))^2 + \gamma_q^2(\omega)} d\omega. \tag{2.34}$$

Eqs. (2.25)–(2.28), (2.33), and (2.34) form a complete set of non-linear equations for six unknowns M_s , P_q , γ_s , γ_q , n_s and ν_q . Strictly speaking, this set must be solved self-consistently. In many realistic situations it is a formidable and impractical task. A way to get around this difficulty can be found by noticing that, when the single-particle damping $\gamma_s(\omega)$ is small, the spectral intensity $J_s(\omega)$ in Eq. (2.32) has a steep maximum at around

$$\tilde{E}_s = E_s + M_s(\tilde{E}_s). \tag{2.35}$$

Expanding $M_s(\omega)$ near this value under the assumption that γ_s is small, it is easy to show that

$$n_s = \frac{1}{\exp(\beta\tilde{E}_s) + 1}. \tag{2.36}$$

Eqs. (2.35) and (2.36) show how the single-particle state is renormalized by the coupling to the phonon field. Eq. (2.36) is the basic assumption in the statistical approach to hot finite and strongly interacting Fermi system, which suggests that the single-particle occupation number can be approximated by a pure Fermi–Dirac distribution with a renormalized energy (See also Ref. [40]). The average value $\Gamma_{s,p}$ of $2\gamma_s$ over all the single-particle levels is calculated as

$$\Gamma_{\text{s.p.}}(\omega) = 2 \frac{\sum_j \Omega_j \gamma_j(\omega)}{\sum_j \Omega_j}, \quad \Omega_j = 2j + 1. \quad (2.37)$$

From Eq. (2.27) it is seen that $\Gamma_{\text{s.p.}}$ grows at high temperatures as $\sim O(T)$ according to Eq. (2.27) (See also Ref. [44]).

If we assume that before the coupling the GDR is generated by a single phonon, associated with a strongly collective vibration at energy ω_q , the full width at half maximum (FWHM) Γ_{GDR} of the GDR, caused by the coupling, is calculated from Eq. (2.28) as

$$\Gamma_{\text{GDR}} = 2\gamma_q(\omega = E_{\text{GDR}}(T)). \quad (2.38)$$

The energy $E_{\text{GDR}}(T)$ of the hot GDR is defined as the pole of the Green function $G_q(\omega)$ in Eq. (2.20), i.e. as the solution of the equation:

$$\omega - \omega_q - P_q(\omega) = 0. \quad (2.39)$$

It is also worth noticing that the structure of Eqs. (2.27) and (2.28) ensues that the effect of single-particle damping on the total width of the GDR is not additive in general.

Let us now examine the evolution of Γ_{GDR} in Eqs. (2.38) and (2.28). At $T = 0$ the single-particle occupation number n_s is equal to 1 for a h state ($E_h < 0$) and 0 for a p one ($E_p > 0$). Therefore Γ_{GDR} has a non-zero value only through the coupling to ph pairs, where $n_h - n_p = 1$. This constitutes the main part of the quantal width Γ^\dagger due to the “ $ph \otimes$ phonon” coupling. With increasing temperature this quantal width, which we denote hereafter as Γ_Q , is expected to decrease as the difference $n_h - n_p$ decreases from 1 at $T = 0$ to 0 at $T = \infty$. At the same time there appear the pp and hh configurations because the difference $n_s - n_{s'}$ differs from zero also for $(s, s') = (p, p')$ or (h, h') at $T \neq 0$. The coupling to the pp and hh configurations leads to the thermal damping Γ_T [35], which increases first with increasing T . However, because of the factor $n_s - n_{s'}$ the total width Γ_{GDR} will decrease as $O(T^{-1})$ at large T . Therefore it must reach some plateau at a certain value of T . The temperature region, where the increase of the phonon damping is slowed down, approaching the plateau, corresponds to the region of the width saturation, observed in the experiments. Just the present formalism is able to provide a natural explanation for the width saturation of the GDR.

We would like to make a point of establishing the connection between the coupling to pp and hh configurations and the thermal shape fluctuations. Namely, in our opinion the coupling to pp and hh configurations may offer an alternative way to take into account thermal shape fluctuations microscopically. To this end, first of all, it is worth noticing that there are several ways to take into account thermal shape fluctuations. A common way is to use a model, in which the motion of nucleons is described in terms of a deformed oscillator, Woods–Saxon or cranked Nilsson potential. The residual interaction between nucleons in the intrinsic system can be described by the dipole-dipole force for the GDR case. This scheme has been proposed in Ref. [22], according to which the cross-section, averaged over all possible thermal fluctuations of shapes, is given by

$$\langle \sigma(E; E^*) \rangle = \frac{\int P(E^*) \sigma(E; E^*) dD}{\int P(E^*) dD}, \tag{2.40}$$

where the excitation energy E^* in general is a function of temperature T , angular momentum I , and deformation parameters β and γ of the system. The probability $P(E^*)$ is proportional to

$$P(E^*) \propto \exp[-F(E^*)/T], \tag{2.41}$$

where $F(E^*)$ is the free energy of the system. The metric dD (volume element) depends on the deformation parameters. In the approach based on the Landau theory of shape transitions [46], the free energy $F(E^*)$ can be expanded in terms of the “deformation” parameters α_{lm} , which determine the deviations of the compound nucleus from the spherical shape. Hence the shape fluctuations must include in general the couplings to all possible multiplicities, not only the quadrupole–quadrupole one. The approach in Ref. [46] then concentrated only on the most important deformation – the quadrupole one, which corresponds to the second order in this expansion α_{2m} , and determined an effective free energy as a function of temperature and α_{2m} only. Another way of taking into account thermal shape fluctuations is based on a model using a collective quadrupole plus GDR Hamiltonian to generate the quadrupole deformation at $T = 0$ [47]. In this case the mean field of oscillator type is deformed already at $T = 0$ with three frequencies ω_i , ($i = x, y, z$), related to the Hill-Wheeler deformation parameters β and γ [37]. This scheme has been applied in the most recent calculations of thermal shape fluctuations with the adiabatic-coupling model in Ref. [25].

In the present formalism the interaction part H_c of the single-particle pairs and the phonon field in Eq. (2.4) includes in general all the multipole-multipole forces with $\lambda \geq 1$. A pp or hh pair operator $B_{ss'} = a_s^\dagger a_{s'}$ can be expanded in the lowest order as a sum of tensor products of ph pair operators: $\sum_h [B_{ph}^\dagger \otimes B_{p'h}]_{\lambda^\pi}$ if $(s, s') = (p, p')$ or $\sum_p [B_{ph'}^\dagger \otimes B_{ph}]_{\lambda^\pi}$ if $(s, s') = (h, h')$ [48]. Therefore the coupling in H_c (Eq. 2.4) can be rewritten, e.g. for the case with $(s, s') = (p, p')$, as

$$H_c \rightarrow H_{BQ} = \sum_{pp'q} F_{pp'}^{(q)} \sum_h [B_{ph}^\dagger \otimes B_{p'h}]_{\lambda^\pi} (Q_q^\dagger + Q_q). \tag{2.42}$$

Expressing B_{ph}^\dagger ($B_{p'h}$) in terms of $Q_{q_1}^\dagger$ and Q_{q_1} ($Q_{q_2}^\dagger$ and Q_{q_2}) using the well-known inverse canonical transformation, one obtains

$$H_{BQ} = \sum_{pp'q_1q_2} F_{pp'}^{(q)} \sum_h \left[(X_{ph}^{(q_1)} Q_{q_1}^\dagger - Y_{ph}^{(q_1)} Q_{q_1}) \otimes (X_{p'h}^{(q_2)} Q_{q_2} - Y_{p'h}^{(q_2)} Q_{q_2}^\dagger) \right]_{\lambda^\pi} (Q_q^\dagger + Q_q). \tag{2.43}$$

Eq. (2.43) suggests that if $Q_{q_1}^\dagger$ and Q_{q_1} are the GDR phonon operators, $\{Q_{q_1}^\dagger, Q_{q_1}\}$ and $\{Q_{q_2}^\dagger, Q_{q_2}\}$ can have the moment and parity as $(1^-, 2^+)$, $(2^+, 3^-)$, etc. so that the total coupled momentum is again equal to $\lambda^\pi = 1^-$. The RPA amplitudes $X_{ph}^{(q_j=\lambda_j, i_j)}$, $Y_{ph}^{(q_j=\lambda_j, i_j)}$ ($j = 1, 2$) in Eq. (2.43) can be calculated microscopically, using the residual

interactions, which include dipole–dipole ($\lambda_j = 1$), quadrupole–quadrupole ($\lambda_j = 2$), octupole–octupole ($\lambda_j = 3$), etc., forces, respectively. This means that the coupling to pp and hh configurations in the term H_c in Eqs. (2.4) and (2.43) in fact already includes, via multiphonon configuration mixing at $T \neq 0$, the coupling to different multipole–multipole fields, not only the dipole–dipole type. In order to avoid confusion, one should notice that the microscopic inclusion of the effects of multiplicities higher than the dipole one is proceeded as follows. First, one solves separately different RPA equations to define the structure of phonons with different multipolarity. Once the structure of these phonons are defined, one couples them to the dipole phonon Q_q^\dagger and Q_q via $F_{ss'}^q$ (with $q = \{\lambda = 1; i\}$) and the phonon amplitudes according to the above mentioned expansion (See, e.g., Ref. [16]). Taking into account the high-lying ph , pp , and hh configurations, as has been discussed above, the coupling to high-lying multiphonon states is also incorporated in our formalism. It is well-known that the configuration mixing of $1p1h$ with $2p2h$ states [16,19] (or ph with phonon ones discussed above (Cf. also Ref. [17])) is decisively important to account for the spreading width Γ^\perp . In addition to the quantal coupling to ph configurations, a quite similar mechanism takes place at $T \neq 0$ via the coupling to pp and hh configurations. As the latter takes place only at $T \neq 0$, it tantamounts to the thermal effects in the fluctuations of multipole deformations of nuclear shapes around the spherical one. We would also like to mention that the division into the “quantal” and “thermal” parts is based purely on the couplings to ph or to pp and hh configurations. The “quantal” part due to the coupling to ph configurations exists at $T = 0$ and its effects are expected to decrease with increasing temperature. The “thermal” part arises from the coupling to pp and hh configurations, which occurs only at $T \neq 0$, and its effects are expected to increase with increasing T .

As has been also mentioned in Ref. [25], a meaningful comparison between theoretical results and the experimental systematics cannot be made without a proper relation between the excitation energy E^* and temperature T . This relation in a finite nuclear system at $T \leq 5$ MeV may deviate noticeably from the description of the Fermi-gas model. In the latter the excitation energy E^* is proportional to the nuclear temperature in square T^2 as

$$E_{\text{F.g.}}^* = aT^2, \quad a = \frac{A}{\alpha}, \quad (2.44)$$

where the level density parameter a can take a value with α varying between around 8 and 12 in heavy nuclei depending on the mass number A . In microscopic calculations using the realistic single-particle energies, the level density parameter $a(T)$ is defined as the half of the derivative of the entropy of the system over the temperature [12,49]. As has been shown in Ref. [50], this microscopic level density parameter $a(T)$ approaches the Fermi-gas value in Eq. (2.44) only in nuclei with a large mass-number A and at a considerably high temperature ($T > 5$ MeV) if the thermal fluctuations are taken into account. As the measurements are usually carried out at a given value of excitation energy E^* , the difference in the definition of excitation energy as a function of temperature may create some uncertainties in the extraction of a corresponding temperature. In

the present paper, besides the excitation energy from the Fermi gas model $E_{F.g.}^*$, we also calculate the excitation energy $E_{m.f.}^*$ of the total system in a microscopic way at each value of temperature T as in Ref. [12,49,50], namely

$$E_{m.f.}^* = \mathcal{E}(T) - \mathcal{E}(T = 0) . \quad (2.45)$$

In Eq. (2.45) $\mathcal{E}(T)$ is the total energy of the system at temperature T , which is calculated in the thermal mean-field as

$$\mathcal{E}(T) = \frac{1}{2} \sum_j \Omega_j \epsilon_j \left[1 - \frac{E_j}{|E_j|} \tanh \left(\frac{1}{2} \beta |E_j| \right) \right] . \quad (2.46)$$

It must be stated that the quantity $E_{m.f.}^*$, defined in Eqs. (2.45) and (2.46), gives just another limit for the excitation energy as compared to the quantity $E_{F.g.}^*$ in Eq. (2.44). In reality there are the effects of residual interactions such as dipole, quadrupole, etc., which are not included in Eq. (2.46). The coefficient K_{vib} for the increase of the level density due to the vibrational modes has been evaluated in Ref. [12] as

$$K_{vib} \simeq \prod_{\lambda_i} \left\{ \frac{[1 - \exp(-\beta \omega_{\lambda_i}^0)]}{[1 - \exp(-\beta \omega_{\lambda_i})]} \right\}^{2\lambda_i + 1} , \quad (2.47)$$

where $\omega_{\lambda_i}^0$ is the ph pole, which corresponds to the RPA solution ω_{λ_i} . In Ref. [50] it has been shown that this coefficient K_{vib} may increase from 1 at $T = 0$ to 1.6 at $T = 2$ MeV under the influence of the quadrupole vibrational modes in ^{58}Ni . This pushes $E_{m.f.}^*$ closer to $E_{F.g.}^*$. Shown in Fig. 1 is the excitation energy $E_{m.f.}^*$ in ^{90}Zr , ^{120}Sn and ^{208}Pb as a function of temperature, using the single-particle energies defined in the Woods–Saxon potential for these nuclei (See Section 3). As seen there is a substantial discrepancy between the value of $E_{m.f.}^*$ and $E_{F.g.}^*$ at $T \leq 5$ MeV. The difference is larger in the lighter system (^{90}Zr), where $E^* > E_{F.g.}^*$, and much reduced in ^{208}Pb , where $E^* < E_{F.g.}^*$ at the same temperature T . As we cannot estimate explicitly the contribution from vibrational modes here, we just show in this figure the arithmetic average $\bar{E}^* = (E_{F.g.}^* + E_{m.f.}^*)/2$ as a function of temperature for a comparison, based on the discussion above.

3. Numerical results

In this section we present the results of a systematic comparison between the calculations within our formalism and the recent experimental data for three nuclei ^{90}Zr , ^{120}Sn and ^{208}Pb as a function of temperature in a wide range $0 \leq T \leq 6$ MeV. We also extend the consideration to higher excitation energies E^* . Since we are interested in the evolution of the hot GDR via its coupling to the single-particle field, a microscopic description of the structure of the g.s. GDR ($T = 0$) and its spreading width Γ^\perp would not be important in the present consideration. Such description can be found in a number of works such as Refs. [16–19]. Moreover the microscopic calculations at $T \neq 0$ [14,20,21] have shown that the GDR can be considered as a strongly collective

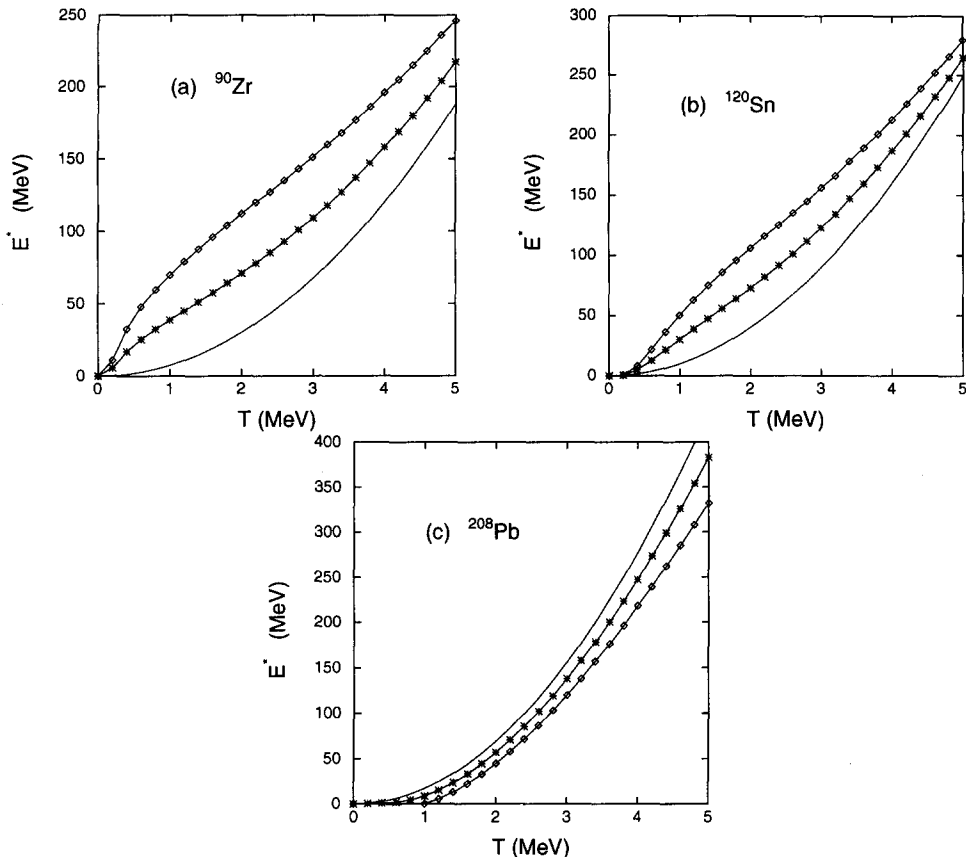


Fig. 1. Excitation energy as a function of temperature. Solid curves with diamonds represent $E_{m.f.}^*$ (see text). Solid curves denotes $E_{F.g.}^*$ of the Fermi-gas model with $\alpha = 12$. Solid curves with stars stands for $\bar{E}^* = (E_{m.f.}^* + E_{F.g.}^*)/2$.

excitation, which is stable against changing the temperature. Therefore in order to have a simple and clear picture, we assume that at the g.s. GDR is generated by a single collective and structureless phonon width energy ω_q closed to the energy E_{GDR} of the g.s. GDR. This GDR phonon is damped via coupling to ph , pp and hh configurations. We employ realistic single-particle energies, calculated in the Woods–Saxon potential at $T = 0$ for ^{90}Zr , ^{120}Sn and ^{208}Pb . The parameters of the Woods–Saxon potentials, used in the calculations, have been defined in Ref. [51]. In ^{208}Pb , in particular, the levels near the Fermi surface are replaced with the empirical ones. The single-particle energies levels span a large region from -30 MeV up to the bound states and quasibound states at around ≤ 20 MeV for both neutron and proton components. This means that after coupling to the GDR phonon the ph -phonon, pp -phonon, and hh -phonon poles in Eq. (2.28) can be located at rather high energies up to more than 50 MeV. The ph , pp and hh poles in the expression for the single-particle damping (Eq. (2.27)) can also be located at up to around 40 MeV. Hence the collective GDR phonon in our

Table 1
Parameters of the model used in calculations

	ω_q (MeV)	F_1 (MeV)	F_2 (MeV)
^{90}Zr	16.8	0.416	1.20
^{120}Sn	17.0	0.313	1.02
^{208}Pb	13.8	0.103	0.548

formalism is practically coupled not only to low lying ph , pp , and hh configurations, but also to high-lying ones. These energies are extended to non-zero temperatures. The self-consistent calculations in the thermal mean-field in Ref. [52] have justified this up to $T \simeq 5\sim 6$ MeV, where the single-particle energies show a little change as a function of temperature. The matrix elements of the coupling to ph and pp or hh are parametrized as $F_{ph}^{(q)} = F_1$ for $(s, s') = (p, h)$ and $F_{pp}^{(q)} = F_{hh}^{(q)} = F_2$ for $(s, s') = (p, p')$ or (h, h') . As the ph interaction in the GDR is dominated only across the two major shells, which are closest to the Fermi surface from both sides, the uniform distribution of the ph strength over all the levels can be justified if $F_1^2 \ll F_2^2$. The phonon energy ω_q , F_1 and F_2 are three parameters in our model. Their values are chosen for each nucleus so that the empirical width Γ_Q and energy E_{GDR} of the g.s. GDR in these nuclei [53] are reproduced after the coupling is switched on, and that the $E_{\text{GDR}}(T)$, defined from Eq. (2.39), does not change appreciably with varying temperature. The best sets of parameters for these nuclei are presented in Table 1. The selected parameters are kept unchanged throughout the calculations at $T \neq 0$. This ensures that all thermal effects are caused by the microscopic coupling between the GDR and the single-particle field, but not by changing parameters. In calculating the damping we use for the δ functions in the RHS of Eqs. (2.27) and (2.28) the representation

$$\delta(x) = \frac{1}{2\pi i} \left(\frac{1}{x - i\varepsilon} - \frac{1}{x + i\varepsilon} \right). \quad (3.1)$$

The results of calculations do not vary appreciably in the interval $0.2 \text{ MeV} \leq \varepsilon \leq 1.0 \text{ MeV}$. Therefore only those, obtained with $\varepsilon = 0.5 \text{ MeV}$, are discussed below.

The average single-particle damping widths $\Gamma_{s,p}$ in ^{120}Sn due to the coupling with the dipole-phonon field are shown in Fig. 2 as a function of temperature. The results are obtained at several values of energy ω below and above E_{GDR} . Comparing Fig. 1a and 1b, one can see clearly that the thermal effects caused by the coupling to pp and hh configurations significantly increase the single-particle damping at $T \neq 0$, especially in the energy region below and near the GDR. The width $\Gamma_{s,p}$ in this region increases non-linearly as increasing temperature from a value around 0.1 MeV at $T = 0$ to around 1.5–1.6 MeV at $T = 5 \text{ MeV}$. In the region above the GDR, $\Gamma_{s,p}$ is rather stable as varying temperature (dash-dotted curves). Its absolute value in this region does not exceed 0.5 MeV. The widths $\Gamma_{s,p}$ in ^{90}Zr and ^{208}Pb show a similar feature. Their absolute values in ^{208}Pb are about two-times smaller than in ^{120}Sn , while they are nearly the same in ^{90}Zr . These results may serve as a good justification for the statistical approximation

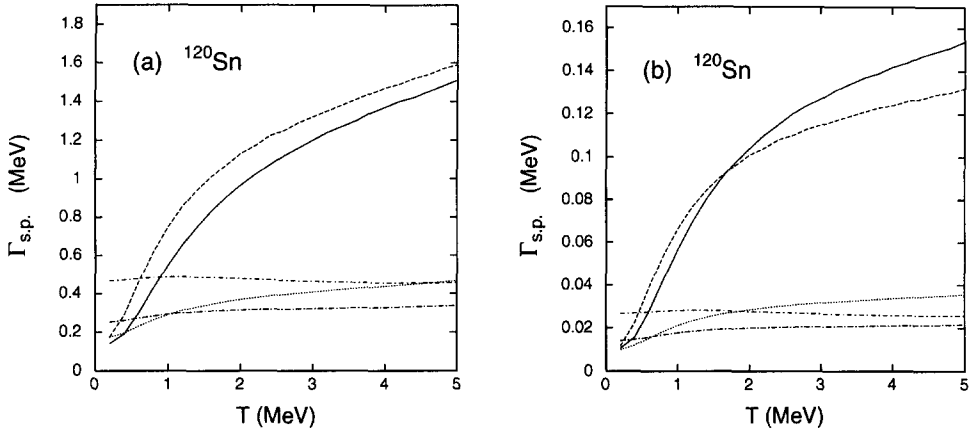


Fig. 2. Average single-particle damping width $\Gamma_{s.p.}$ in ^{120}Sn as a function of temperature. (a) Results through the coupling to all ph , pp and hh configurations; (b) Results through the coupling to only ph configurations. Solid, dashed, dotted, long dash-dotted and short dash-dotted curves are obtained with $\omega = E_{\text{GDR}} - \Delta E$, where $\Delta E = 2, 1, 0, -1$ and -2 , respectively.

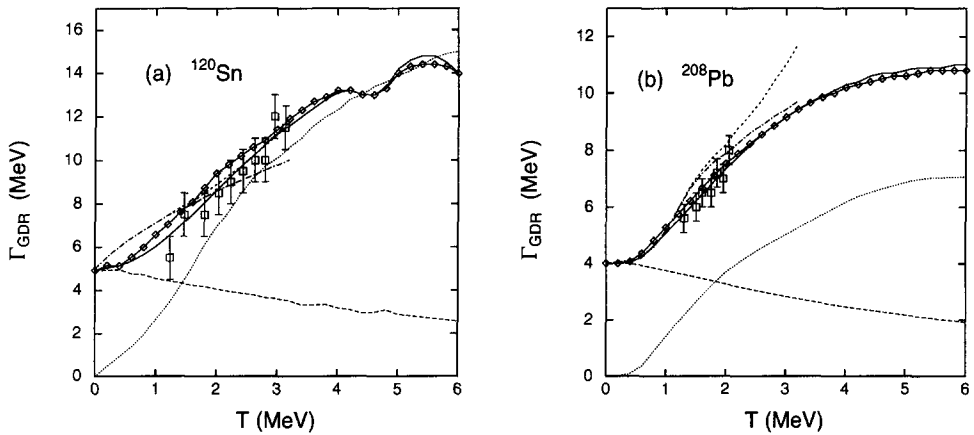


Fig. 3. Width of GDR as a function of temperature for ^{120}Sn (a) and ^{208}Pb (b). Experimental data of Ref. [10] are shown by open squares. The dashed curve denotes the quantal width Γ_Q ; the dotted curve stands for thermal width Γ_T ; the solid curve with diamonds represents the total width Γ_{GDR} (See text). The solid curve is Γ_{GDR} , calculated without the effect of single-particle damping. The dash-dotted and short dashed curves represent the widths obtained within the adiabatic model [11] without and including the evaporation width, respectively.

based on Eq. (2.36). Taking into account the coupling to other multipolarities increases the total single-particle damping width to around 1 MeV at $T = 0$ and 2–3 MeV at $T = 3$ MeV, as has been shown by Donati et al. in Ref. [54].

The FWHM of the GDR and its components, calculated from Eq. (2.38) in ^{120}Sn and ^{208}Pb are displayed as a function of temperature in Fig. 3 in comparison with the recent inelastic α scattering data [11]. The quantal width Γ_Q (dashed curve) is obtained through the coupling to only ph states. The thermal width Γ_T (dotted curve)

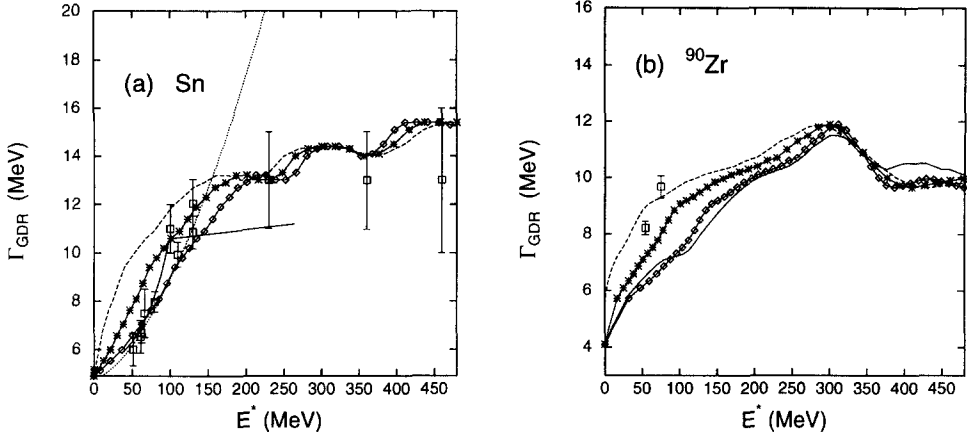


Fig. 4. Width of GDR in Sn (a) and ^{90}Zr (b) as a function of excitation energy. Experimental FWHM from Refs. [3-6,9] (a) and Ref. [7] (b) are represented by open squares. The solid with diamonds represents the width Γ_{GDR} in our model, plotted as a function of $E_{\text{m.f.}}^*$. The dashed curve is the same width, but plotted as a function of $E_{\text{F.g.}}^*$. The solid curve with stars is the same width, plotted as a function of \bar{E}^* (See text). In (b) the solid curve is the width Γ_{GDR} , calculated without the effect of single-particle damping and plotted against $E_{\text{m.f.}}^*$. In (a) the width, obtained in Ref. [24], is represented by the solid curve, while the result of Ref. [28] is shown by the dotted curve.

comes from the coupling to pp and hh configurations at $T \neq 0$. The total width Γ_{GDR} (solid-with-diamond curve) is calculated through the coupling to all ph , pp and hh configurations, including the effect of single-particle damping. In general, Γ_{GDR} is not the sum of Γ_Q and Γ_T because the poles of the Green function $G_q(\omega)$ are different due to the coupling to different configurations. It is clear from this figure that the quantal effects become weaker in hot GDR as Γ_Q is getting smaller slowly with T going up. A slightly smaller width of GDR at $T = 3$ MeV in ^{90}Zr and ^{208}Pb has also been reported in the numerical calculations within the NFT in Ref. [20]. The thermal damping width Γ_T , on the contrary, becomes rapidly larger as increasing T . As the result, Γ_{GDR} increases sharply as T raises up to 3 MeV and slowly at higher temperatures. It reaches a saturated value of around 14 MeV in ^{120}Sn and 11 MeV in ^{208}Pb at $T = 4-6$ MeV. The behavior of the width as a function of T is different in two nuclei. The reason comes from the difference in the single-particle energies between nuclei. These evaluations show that the GDR width at high temperatures is driven mostly by the thermal width Γ_T . The results of our calculations agree well with the experimental data. This agreement is also better than the one given recently within the adiabatic model in Ref. [25]. Our results also cover a much wider temperature region. The effect of the single-particle damping is rather small up to very high temperature (Compare the solid-with diamonds and solid curves).

Shown in Fig. 4 is the same width Γ_{GDR} in our model for ^{120}Sn and ^{90}Zr , but plotted as a function of excitation energy E^* in comparison with the FWHM of the GDR from the heavy-ion fusion data in tin isotopes [3-6,9] and in ^{90}Zr [7]. An overall agreement between our results and the experimental data is seen in the whole region of

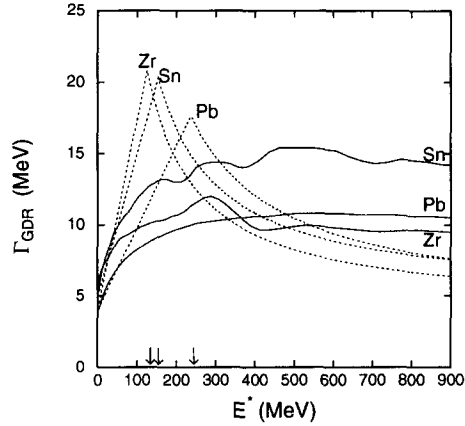


Fig. 5. Width Γ_{GDR} as a function of Fermi-gas excitation energy $E_{\text{F.g.}}^*$. The solid curves represent Γ_{GDR} in ^{90}Zr , ^{120}Sn and ^{208}Pb . The dotted curves denote the corresponding widths $\Gamma_{<}$ and $\Gamma_{>}$ from the Landau theory of Fermi liquid [27]. The arrow shows the energy of the phase transition point, which is 126, 154 and 237 MeV for $A = 90, 120$ and 208 , respectively.

excitation energy E^* , including the data at $250 \leq E^* \leq 450$ MeV [4]. The predictions of Refs. [24] (solid curve) and [29] (dotted curve) are also shown. They are similar to ours at $E^* \leq 150$ MeV. In this region there is a large discrepancy between the dependence of Γ_{GDR} on $E_{\text{m.f.}}^*$ from Eq. (2.45) (solid with diamonds) [50] and the one on $E_{\text{F.g.}}^*$ (dashed). The same width plotted as a function of $\bar{E}^* = (E_{\text{m.f.}}^* + E_{\text{F.g.}}^*)/2$ is also shown in Fig. 4 for comparison. This discrepancy is the reason why theory underestimates the data in ^{90}Zr if plotted versus $E_{\text{m.f.}}^*$, while it is found in a more reasonable agreement with the data if plotted versus $E_{\text{F.g.}}^*$ (Fig. 4b).

The dependence of the same width Γ_{GDR} as a function of $E_{\text{F.g.}}^*$ in a much larger region up to $E_{\text{F.g.}}^* = 900$ MeV is represented in Fig. 5. The width saturation is clearly seen in all three nuclei starting from $E^* \sim 150$ MeV. According to the Landau theory of Fermi liquids [28] the behavior of vibrations of a Fermi liquid at $T \neq 0$ is different depending on the relaxation time $\tau \sim \Gamma^{-1}$. The region where the frequency $\omega \gg \Gamma$ corresponds to the region of zero-sound propagation (the collisionless or rare-collision regime), while the ordinary sounds takes place if $\omega \ll \Gamma$ (the frequent-collision regime). The absorption coefficient (damping) γ is $\propto T^2$ in the zero-sound region and $\propto \omega^2/T^2$ in the ordinary-sound region. The transitional region $\omega \sim \Gamma$ corresponds to a very strong absorption, where the isolation of the different types of waves as undamped processes is not possible. As the g.s. GDR can be considered as an analogue of the zero sound (with a certain damping) in finite systems, the following widths can be deduced for the damping of the GDR at $T \neq 0$ in the zero-sound region:

$$\Gamma_{<} = \Gamma_{\text{GDR}}^{T=0} + c_1 T^2 \quad \text{if} \quad \Gamma_{\text{GDR}} \ll E_{\text{GDR}}, \quad (3.2)$$

and ordinary-sound region:

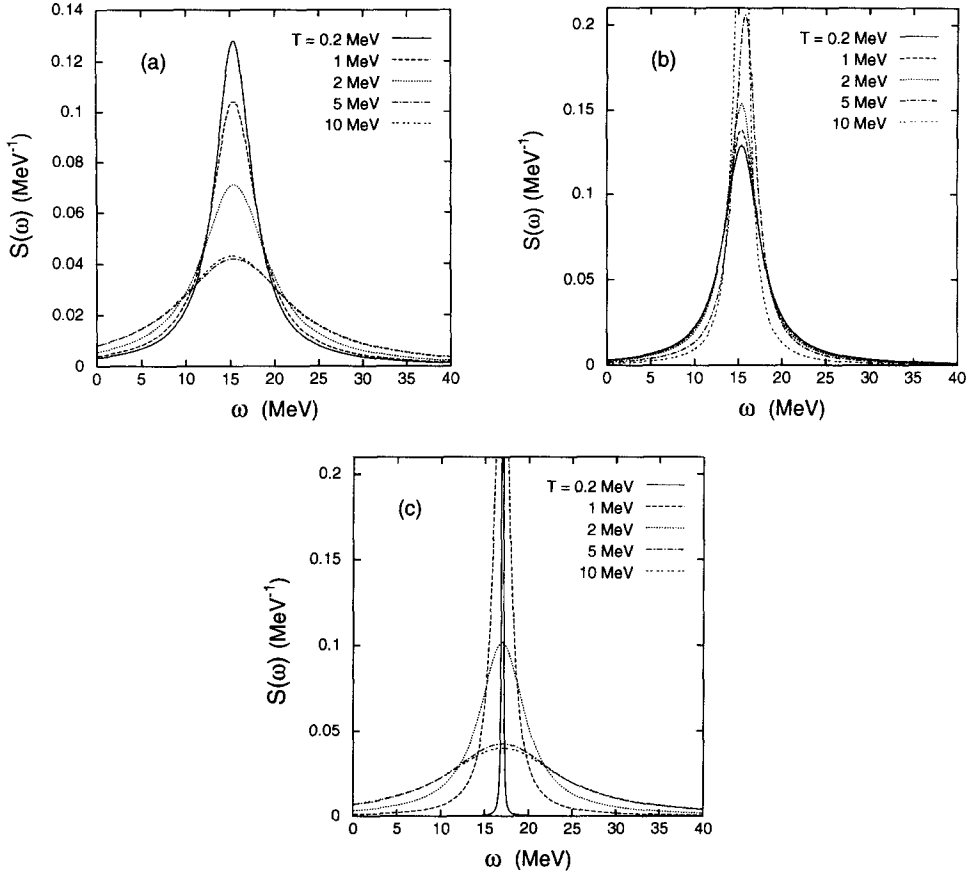


Fig. 6. Strength function $S_{\text{GDR}}(\omega)$ of the GDR in ^{120}Sn at several temperatures. (a) Results, obtained via the coupling to all ph , pp and hh configurations. (b) Results, obtained via the coupling to only ph configurations. (c) Results, obtained via the coupling to pp and hh configurations.

$$\Gamma_{>} = \Gamma_{\text{GDR}}^{T=0} + c_2 \left(\frac{E_{\text{GDR}}}{T} \right)^2 \quad \text{if } \Gamma_{\text{GDR}} \gg E_{\text{GDR}}. \quad (3.3)$$

This behavior would correspond to the transition from the quantal region (zero-sound) to the region of a full thermodynamic equilibrium (ordinary sound). The widths $\Gamma_{>}$ and $\Gamma_{<}$ with $c_1 = 1 \text{ MeV}^{-1}$ and $c_2 = 1 \text{ MeV}$ are also plotted in Fig. 6 with a phase transition point at $T \simeq 4.1, 3.9$ and 3.7 MeV for the system with $A = 90, 120,$ and 208 , respectively. It is seen from this figure that the behavior of the GDR width in ^{90}Zr , ^{120}Sn and ^{208}Pb exhibits a similar feature to the transition from zero to ordinary sounds in a Fermi liquid, although the phase transition is strongly smeared out in hot nuclei. Hence the region of width saturation in finite nuclei may correspond to the transitional region in the hot Fermi liquid, where the two sounds cannot be separated as they are both strongly overdamped. According to what discussed above, the dominating contribution in the GDR width in finite nuclei at $T = 0$ and very low T comes from the coupling of the collective phonon to ph configurations, while at high T the GDR width is constituted mainly by the coupling

Table 2

The value $\Delta E_j = \tilde{E}_j - E_j$ for several levels near the Fermi surface in ^{208}Pb at $T = 10$ MeV

Z		N	
<i>nlj</i>	ΔE_j (MeV)	<i>nlj</i>	ΔE_j (MeV)
1g _{7/2}	-0.483	1h _{9/2}	0.0063
2d _{5/2}	0.424	2f _{7/2}	-0.397
1h _{11/2}	0.174	1i _{13/2}	0.383
2d _{3/2}	-0.006	3p _{3/2}	0.402
3s _{1/2}	-0.330	2f _{5/2}	0.142
1h _{9/2}	-0.105	3p _{1/2}	-0.335
2f _{7/2}	0.299	2g _{9/2}	-0.003
1i _{13/2}	0.231	1i _{11/2}	0.554
2f _{5/2}	-0.006	1j _{15/2}	0.415
3p _{3/2}	-0.007	3d _{5/2}	0.328
3p _{1/2}	0.330	4s _{1/2}	0.007

to pp and hh . If we recall that in the fully microscopic description the particle–phonon coupling term H_c in Eq. (2.4) in fact includes the configuration mixing between phonon excitations with different multipolarities (Eq. (2.43)), the multiparticle collisions are indeed already included in H_c . In the numerical calculations in the present work these collisions are effectively taken into account by choosing the parameters F_1 and F_2 . The increase of thermal effects due to the coupling to pp and hh as increasing temperature, therefore, corresponds directly to the increase of collisions. This leads to a transition from a rare collision regime at low temperature, where the quantal effects are dominated (coupling to ph configurations), to a frequent collision regime at high temperature, which is driven mostly by thermal effects (coupling to pp and hh configurations). Therefore we conclude that the quantal effects of coupling to ph configurations in finite nuclei create an analogue of the damping of zero sound, while the thermal effects due to the coupling to pp and hh correspond to the appearance of ordinary sound in hot nuclear matter. We also found that the effect of single-particle damping is rather small up to very high temperature. An example is given in Table 2, where the values of the difference $\Delta E_j = \tilde{E}_j - E_j$ with \tilde{E}_j being the solution of Eq. (2.35) for the levels around the Fermi surface in ^{208}Pb at $T = 10$ MeV are shown. We should not forget that other effects, such as the temperature-dependence of the single-particle energies, the influence of higher multipolarities on the single-particle damping, the explicit coupling to the continuum, the inclusion of the evaporation width, etc., which are left out in this study, may also improve the results in this region of very high excitation energy. By the same reason, the correspondence between the zero-to-ordinary sound transition in the Fermi liquid and the behavior of the hot GDR width, calculated within our formalism, must be understood in this context.

The propagation of zero sound in excited nuclear matter has been also discussed within the Landau–Vlasov formalism in Ref. [30], where the transition from zero to ordinary sounds has been referred to as a possible mechanism of the “disappearance” of GDR at

high temperatures. This mechanism can be interpreted based on the results obtained in this work as follows. Shown in Fig. 6 is the strength function $S_{\text{GDR}}(\omega)$, calculated from Eq. (2.32), in ^{120}Sn at several temperatures for a GDR centered at $E_{\text{GDR}}(T)$ with the width Γ_{GDR} , obtained above. The quantal coupling to ph configurations (Fig. 6b) makes the GDR peak narrower (Cf. [20]), while the thermal effects due to the coupling to pp and hh configurations (Fig. 6c) enlarges the GDR as increasing temperature. Higher than $T \sim 3\text{--}4$ MeV the peak, caused by thermal effects alone, ceases to change as its width reaches a saturation. The combined effects (Fig. 6a) give a GDR peak, which changes drastically when increasing T up to $3\text{--}4$ MeV, but becomes temperature-independent at higher T , conserving the total GDR strength. Already in Ref. [35], it has been shown in a simplified model that there is an energy dissipation from the peak in Fig. 6b to the one in Fig. 6c. We can see here that the realistic situation is driven by the same mechanism. The difference is that the space of pp and hh configurations in realistic hot nuclei is significantly larger and spreads up to high energies including the GDR region and beyond it. This makes the GDR persists even up to very high temperature ($T = 10$ MeV in the figure) with all its strength preserved. Hence the hot GDR does not seem to disappear within the present model. This result must be understood in the context that the damping mechanism of the GDR at high temperatures mostly comes from thermal effects via the coupling to pp and hh configurations. The quantal effects through the coupling to ph states, which are responsible for the damping of the g.s. GDR as zero sound, vanishes at high temperatures. As has been noticed in Ref. [8], there is no evident discrepancy between the γ spectra measured in the various experiments, rather the methods of analysis seem to lead to contradictory conclusions. One of the reasons, as has been mentioned above, may be the uncertainties in the experimentally extracted temperature. In order to show this more clearly, we notice that the measured γ absorption cross-section is proportional to the spectral intensity $J_q(\omega)$ in Eq. (2.32). In order to recover the GDR strength function $S_q(\omega)$ the spectral intensity must be multiplied by $(\exp(\omega/T) - 1)$. In practice, after subtracting the back ground, the γ ray spectra are usually extracted in the experiments by multiplying the total-window γ -ray spectra with $\exp(\omega/T_{\text{eff}})$, where T_{eff} is an effective temperature, characterizing the average excitation energy E^* of the system. If the value of T_{eff} does not coincide with the value T , it can affect the extracted result. An example is shown in Fig. 7 for the spectral intensity $J_q(\omega)$ of the GDR in ^{120}Sn at $T = 3$ MeV after multiplying it by $\exp(\omega/T)$ (solid curve). If T_{eff} was taken from the Fermi-gas model (Eq. (2.44)), it would equal to $T_{\text{eff}} \simeq 4$ MeV at the same value of excitation energy because $E_{\text{m.f.}}(T = 3 \text{ MeV}) \simeq E_{\text{F.g.}}(T_{\text{eff}} = 4 \text{ MeV})$ (Fig. 1b). This would lead to a less collective GDR peak as shown by the dashed line in Fig. 7. This artifact shows up only at intermediate temperatures $1 \leq T \leq 3\text{--}4$ MeV ($100 \leq E_{\text{F.g.}}^* \leq 160$ MeV), where the discrepancies are largest. At higher temperatures or in very heavy nuclei these uncertainties are much reduced since $E_{\text{m.f.}}^* \simeq E_{\text{F.g.}}^*$.

Finally we would like to notice that the mechanism of the “disappearance” of the hot GDR at very high temperature is, nonetheless, still being debated. Following the interpretation of Ref. [45], the particle evaporation width Γ_{ev} should also lead to a maximum excitation energy (or limiting temperature) above which the GDR is not

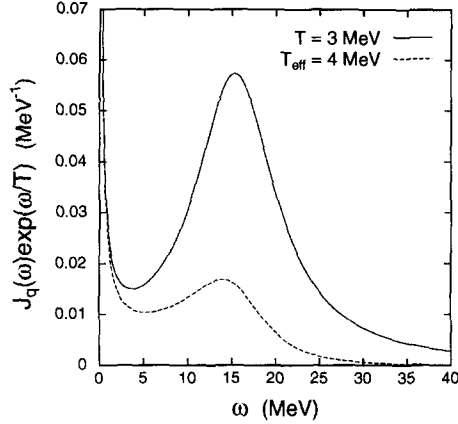


Fig. 7. Spectral intensity $J_q(\omega)$ of the GDR in ^{120}Sn at $T = 3$ MeV, multiplied by $\exp(\omega/T)$ (solid curve) and by $\exp(\omega/T_{\text{eff}})$ (dashed curve).

observable. The similar argument has been proposed in Ref. [26], according to which the GDR width should reach a value around 30 MeV at the excitation energy $E^* \simeq 400$ MeV. However, the same Ref. [26] has also pointed out that, in order to fit the existing experimental data, one needs to introduce an explicit suppression of the GDR strength when the nucleus reaches an excitation energy around 300 MeV [55]. In such a case, the question of the GDR width may become irrelevant above the excitation energy where its strength vanishes or becomes too small. There are two reasons why we leave these question for further studies. First, even though the contribution of the continuum is effectively included in our calculations via the high-lying discrete states, the explicit inclusion of the continuum is beyond the framework of the present formalism. As has been mentioned in Section 1 [14], it is clear that the escape width is almost independent of temperature. Nevertheless, an extension of an approach such as the one in Ref. [56] to take into account the continuum at $T \neq 0$ is called for. Apart from this, the energy weighted sum rule for the GDR is well conserved within our approach. Second, as has been proposed by the author of Ref. [26], the predicted rapid increase of the GDR width due to the particle evaporation at very high temperatures should be experimentally tested. Existing experimental data from heavy-ion fusion reactions so far indicate on a saturation, rather than an increase, of the GDR width in tin isotopes at $E^* \geq 250$ MeV in agreement with theoretical estimation within our formalism. The authors of Ref. [9], on the other hand, have also demonstrated that, the spectra, obtained by them, can be reproduced with or without a saturation of the width providing that it reaches large values, of the order of 15 to 20 MeV, above 100 MeV of excitation energy. Our calculations have shown that Γ_{GDR} in ^{120}Sn actually reaches a value ~ 14 MeV at $E^* \geq 300$ MeV, which matches this criterion in favor of the width saturation. This discussion simply shows that the question of the behavior of the hot GDR at very high temperatures needs further investigations both experimental and theoretical.

4. Conclusions

In this paper we have presented an approach to a systematic theoretical study of the width of the GDR as a function of temperature in the nuclei ^{90}Zr , ^{120}Sn , and ^{208}Pb . The results have been compared with the recent experimental data of the GDR width in heavy-ion fusion reactions as well as inelastic α scattering. An overall agreement between theory and experiment is found in a large region of excitation energies up to $E^* \sim 450$ MeV, where the heavy-ion fusion data are currently available. For the first time the theory describes both regions of the width's increase as well as the width's saturation in a uniform way.

The analysis in the present paper can be summarized as follows:

- (i) The double-time Green function method is a powerful tool to derive a consistent microscopic approach to the damping of the GDR in a large region of excitation energy since the advanced and retarded double-time Green functions can be continued analytically in the complex-energy plane.
- (ii) Thermal effects due to the coupling of the GDR collective vibration to the pp and hh configurations play indeed a decisive role in the increase of the GDR's width at low excitation energies (up to 130–150 MeV) and in the width's saturation at high excitation energies. It seems that the effects of coupling to pp and hh configurations, including high-lying levels in the continuum region, are fairly enough to account for the thermal fluctuations in the hot GDR in finite nuclei. The quantal width Γ_Q , which is caused by the coupling of the GDR to only ph configurations, decreases slowly with increasing temperature T . The region where the GDR width saturates can serve as an analogue of a gradual transition from zero sound (g.s. GDR) to ordinary sound (hot GDR) in finite nuclei at non-zero temperature.
- (iii) The present formalism is based on the assumption of the small single-particle damping. The validity of this assumption is confirmed by the present numerical calculations in hot realistic nuclei, which show that the effects of single-particle damping on the GDR width are small up to very high temperatures even with the scattering term included. This can serve as a good justification for using the Fermi–Dirac distribution to describe the single-particle occupation number as has been usually assumed in statistical approaches to hot nuclei. If the single-particle damping is large, the approximation in Eq. (2.36) is no more valid. In this case one has to solve the set of Eqs. (2.25)–(2.28), (2.33), and (2.34) self-consistently. This may be the case, e.g. when one attempts to take into account the contribution of the coupling to the continuum rigorously in the damping of the GDR at very high temperatures. This question, however, requires further theoretical as well as experimental studies. In particular, the issue on the “disappearance” of the hot GDR is still offering plenty of room for debates [30,45]. At least, the point should be to prove more clearly on what is the mechanism of this “disappearance”: the rapid increase of the evaporation width [45] or the width saturation, which may correspond to the zero-to-ordinary sound transition, as has been shown in the present work and also discussed in Ref. [30], or both of them. It is our hope that,

in the future study of this issue, the results obtained in the present work can serve as one of useful guidelines.

- (iv) A more detail study on the relation between the excitation energy and temperature in finite nuclei at temperatures below $T = 5$ MeV is called for in order to avoid the uncertainties in confronting theoretical predictions and the data. The contribution from collective vibrational modes, which may enhance the level density [50], and from other sources may have to be included to improve the results.

The application of the present formalism to the case, when the GDR consists of more than one collective phonon, is straightforward. The structure of phonons can be then defined from a microscopic Hamiltonian within the RPA as in Refs. [16,17]. Hence one can calculate the parameters of the model rather than choosing them empirically at $T = 0$. While this will certainly make the numerical calculations much more complicate, it will not alter the conclusions above since the physics of thermal damping is independent of this procedure.

Acknowledgements

Numerical calculations were carried out by a 64-bit Alpha AXP work-station running Digital UNIX (OSF/1) at the Computer Center of RIKEN. The authors are grateful to A. Mengoni, N. Onishi, K. Tanabe and S. Yamaji for fruitful discussions. N.D.D. thanks the financial support of the Science and Technology Agency of Japan.

References

- [1] K. Snover, *Ann. Rev. Nucl. Part. Sci.* 36 (1986) 545;
J.J. Gaardhøje, *Ann. Rev. Nucl. Part. Sci.* 42 (1992) 483.
- [2] J.L. Egido and P. Ring, *J. Phys. G* 19 (1993) 1.
- [3] J.J. Gaardhøje et al., *Phys. Rev. Lett.* 53 (1984) 148; 56 (1986) 1783.
- [4] J.J. Gaardhøje et al., *Phys. Rev. Lett.* 59 (1987) 1489.
- [5] D.R. Chakrabarty et al., *Phys. Rev. C* 36 (1987) 1886.
- [6] A. Bracco et al., *Phys. Rev. Lett.* 62 (1989) 2080.
- [7] J.H. Gundlach et al., *Phys. Rev. Lett.* 65 (1990) 2523.
- [8] J.H. Le Faou et al., *Phys. Rev. Lett.* 72 (1994) 3321.
- [9] D. Perroutsakou et al., *Nucl. Phys. A* 600 (1996) 131.
- [10] A. Bracco et al., *Phys. Rev. Lett.* 74 (1995) 3748.
- [11] E. Ramakrishnan et al., *Phys. Rev. Lett.* 76 (1996) 2025.
- [12] A.V. Ignatyuk, *Izv. Acad. Nauk SSSR (ser. fiz.)* 38 (1974) 2613;
A.V. Ignatyuk, *Statistical Properties of Excited Atomic Nuclei (Energoatomizdat, Moscow, 1983)*.
- [13] D. Vautherin and N. Vinh Mau, *Phys. Lett. B* 120 (1983) 261; *Nucl. Phys. A* 422 (1984) 140.
- [14] H. Sagawa and G.F. Bertsch, *Phys. Lett. B* 146 (1984) 138.
- [15] N. Dinh Dang, *J. Phys. G* 11 (1985) L125.
- [16] V.G. Soloviev, *Theory of Atomic Nuclei – Quasiparticles and Phonons (Energoatomizdat, Moscow, 1989)*.
- [17] G.F. Bertsch, P.F. Bortignon and R.A. Broglia, *Rev. Mod. Phys.* 55 (1983) 287.
- [18] S. Drożdż et al., *Phys. Rep.* 197 (1990) 1.
- [19] K. Takayanagi, K. Shimizu and A. Arima, *Nucl. Phys. A* 447 (1988) 205; A 481 (1988) 313.
- [20] P.F. Bortignon et al., *Nucl. Phys. A* 460 (1986) 149.

- [21] N. Dinh Dang, Nucl. Phys. A 504 (1989) 143.
- [22] M. Gallardo et al., Nucl. Phys. A 443 (1985) 415.
- [23] N. Dinh Dang, J. Phys. G 16 (1990) 623.
- [24] R.A. Broglia, B.F. Bortignon and A. Bracco, Prog. Part. Nucl. Phys. 28 (1992) 517.
- [25] W.E. Ormand, P.F. Bortignon and R.A. Broglia, Phys. Rev. Lett. 77 (1996) 607;
W.E. Ormand et al., Nucl. Phys. A 614 (1997) 217.
- [26] Ph. Chomaz, Phys. Lett. B 347 (1995) 1.
- [27] M. Matuszewska et al., Nucl. Phys. A 612 (1997) 262.
- [28] L.D. Landau, Sov. Phys. JETP 5 (1957) 101.
- [29] A. Bonasera et al. Nucl. Phys. A 569 (1994) 215c.
- [30] V. Baran et al., Nucl. Phys. A 599 (1996) 29c.
- [31] V.M. Kolomietz, V.A. Plujko and S. Shlomo, Phys. Rev. C 52 (1995) 2480.
- [32] Y. Alhassid, B. Bush and S. Levit, Phys. Rev. Lett. 61 (1988) 1926;
Y. Alhassid and B. Bush, Nucl. Phys. 509 (1990) 461; A 531 (1991) 1; A 531 (1991) 39;
B. Bush and Y. Alhassid, Nucl. Phys. A 531 (1991) 27.
- [33] B. Lauritzen et al., Phys. Lett. B 207 (1988) 238.
- [34] N. Dinh Dang, in Second Europ. Biennial Conf. on Nuclear Physics, Megève, 1993, ed. D. Guinet (World Scientific, Singapore, 1995) p. 155;
N. Dinh Dang and M. Baldo, in Perspectives of Nuclear Physics in the Late Nineties, Hanoi, 1994, ed. N. Dinh Dang, D.H. Feng, N. Van Giai and N. Dinh Tu (World Scientific, Singapore, 1995) 212;
N. Dinh Dang, Phys. Rep. 264 (1996) 123.
- [35] N. Dinh Dang and F. Sakata, Phys. Rev. C 55 (1997) 2872.
- [36] N. Vinh Mau, Nucl. Phys. A 548 (1992) 381.
- [37] D.M. Brink, Nucl. Phys. 4 (1957) 215;
A.V. Ignatyuk and I.N. Mikhailov, Sov. J. Nucl. Phys. 33 (1981) 919;
K. Neergard, Phys. Lett. B 110 (1982) 7;
P. Ring et al., Nucl. Phys. A 419 (1984) 261.
- [38] N. Dinh Dang and V.G. Soloviev, JINR Communication P4-83-325 (Dubna, 1983) 14p (in Russian).
- [39] V.V. Voronov et al., Sov. J. Nucl. Phys. 40 (1984) 438.
- [40] V. Zelevinsky et al., Phys. Rep. 276 (1996) 85.
- [41] N.N. Bogolyubov and S. Tyablikov, Sov. Phys. Doklady 4 (1959) 6.
- [42] D.N. Zubarev, Sov. Phys. Uspekhi 3 (1960) 320.
- [43] A.A. Abrikosov, A.P. Gorkov and I.E. Dzialoshinsky, Methods of Quantum Field Theory in Statistical Physics (Pergamon, New York, 1963).
- [44] P. Donati et al., Phys. Lett. B 383 (1996) 15.
- [45] P.F. Bortignon et al., Phys. Rev. Lett. 67 (1991) 3360.
- [46] S. Levit and Y. Alhassid, Nucl. Phys. A 413 (1984) 439;
Y. Alhassid, J. Zingman and S. Levit, Nucl. Phys. A 469 (1987) 205.
- [47] J.M. Eisenberg and W. Greiner, Nuclear Theory (North-Holland, Amsterdam, 1975), Vol. I, Chap. 10 and 11.
- [48] F. Catara, N. Dinh Dang and M. Sambataro, Nucl. Phys. A 579 (1994) 1.
- [49] L.G. Moretto, Phys. Lett. B 40 (1972) 1; Nucl. Phys. A 182 (1972) 641.
- [50] N. Dinh Dang, Z. Phys. A 335 (1989) 253.
- [51] V.A. Chepurinov, Sov. J. Nucl. Phys. 6 (1967) 955;
K. Takeuchi and P.A. Moldauer, Phys. Lett. B 28 (1969) 384;
V.G. Soloviev et al., Nucl. Phys. A 228 (1977) 376.
- [52] M. Brack and P. Quentin, Phys. Lett. B 52 (1974) 159;
P. Bonche, S. Levit and D. Vautherin, Nucl. Phys. A 427 (1984) 278.
- [53] B.L. Berman and S.C. Fultz, Rev. Mod. Phys. 47 (1975) 713.
- [54] P. Donati, P.F. Bortignon and R.A. Broglia, Z. Phys. A 354 (1996) 249.
- [55] A. Smerzi, A. Bonasera and M. Di Toro, Phys. Rev. C 44 (1991) 1713.
- [56] Nguyen Van Giai and Ch. Stoyanov, Phys. Lett. B 252 (1990) 9;
G. Colò et al., Phys. Lett. B 276 (1992) 279;
Nguyen Van Giai, Ch. Stoyanov and V.V. Voronov, Nucl. Phys. A 599 (1996) 271c.